Check for updates

Petrale sole transboundary connectivity and settlement success: a biophysical approach

Francisco Santa Cruz[1]*, Carolina Parada[2,3], Melissa Haltuch[4], John Wallace[4], Sebastián Cornejo-Guzmán[2] and Enrique Curchitser[5]

[1]Departamento Científico, Instituto Antártico Chileno, Punta Arenas, Chile, [2]Departamento de Geofísica, Universidad de Concepción, Concepción, Chile, [3]Center for Ecology and Sustainable Management of Oceanic Islands (ESMOI), Departamento de Biología Marina, Facultad de Ciencias del Mar, Universidad Católica del Norte, Coquimbo, Chile, [4]Fishery Research Analysis and Monitoring Division, Northwest Fisheries Science Center, National Marine Fisheries Service, National Oceanic and Atmospheric Administration, Seattle, WA, United States, [5]Department of Environmental Sciences, Rutgers University, New Brunswick, NJ, United States

Connectivity between inferred spawning areas and potential settlement areas of the petrale sole (*Eopsetta jordani*) was explored in the California Current System (CCS) using an individual-based model (IBM) coupled with the ROMS hydrodynamic model for the period 1988-2008. The IBM modeled pelagic early life stages, including egg and larval development, growth, natural mortality and settlement into benthos. Eggs were released within discrete spawning grounds identified from the winter fishery logbook data. Potential settlement areas were defined based on bathymetrical criteria and juvenile (2-year old) distribution from a groundfish bottom trawl survey. The influence of cross-shelf and alongshore advection on the transport and connectivity between spawning and benthic settlement areas was explored by identifying the location of juveniles (22 mm length) among the potential settlement areas. The most important spawning regions varied over time with between 4 and 19% of spawned individuals successfully settling, mostly ranging from off northern Washington to northern Oregon. The strong influence of northward alongshore transport resulted in transboundary transport of pelagic life stages from U.S. spawning grounds to inner shelf settlement areas in Canadian waters, with 33.9-70.4% (average 49.7 ± 9.6) of annual successful juveniles settling in Canada. Interannual variability in juvenile settlement success suggests that mesoscale (100-200 km) oceanographic structures play a major role defining pelagic juvenile transport trajectories. While, in some years, the presence of coastal cyclonic eddies can retain juveniles off Oregon, the strong northward transport supplies a large number of juveniles to Moresby and Vancouver island, clearly showing that petrale sole off the west coast of North America are a transboundary stock with important settlement areas off the coast of British Columbia, thus extension of this study into Canadian waters is particularly relevant.

KEYWORDS

California current, *Eopsetta jordani*, petrale sole, settlement, connectivity, transboundary

Introduction

Transboundary species pose challenges for fisheries management due to uncertainty around stock dynamics from individual management actions that may have disproportionate impacts on stock trends (Thebaud, 1997). Ineffective international collaborations increase risk to shared stock resources (Campana, 2016), especially under current climate change (Palacios-Abrantes et al., 2020a), where catches of transboundary species that are managed independently are more likely to decline compared to non-transboundary species due to national level policies rather than international collaborations that better maximize long-term ecological, social and economic benefits (Palacios-Abrantes et al., 2020b).

While a few northeast Pacific transboundary groundfish stocks shared between the U.S. and Canada are subject to formal management arrangements (e.g. Pacific hake *Merluccius productus* and Pacific halibut *Hippoglossus stenolepis*), there are many more transboundary stocks for which both science and management are largely independent. Petrale sole (*Eopsetta jordani*, Pleuronectidae), the most commercially valuable flatfish targeted in the California Current System (CCS), is one such resource. The degree of stock connectivity between the U.S. and Canada is uncertain given the lack of genetic studies or research on stock structure. However, common trends in abundance and similar life history characteristics have long led to suggestions that petrale sole comprise a transboundary stock (Ketchen and Forester, 1966; Starr and Fargo, 2004; Starr, 2009; Haltuch et al., 2013). Additionally, the possibility for natal homing with some mixing between different spawning groups to known spawning grounds (Di Donato and Pasquale, 1970; Pedersen, 1975) that span both U.S. and Canadian waters of the CCS suggests some transboundary connectivity. During pelagic life stages, it is likely that drift of eggs, larvae, and pelagic juveniles result in an unknown degree of transboundary population connectivity.

The petrale sole fishery experienced a rapid expansion at the close of World War II into the 1950s, with substantial portions of the annual harvest in both U.S. and Canadian waters taken from localized winter spawning aggregations (Alverson and Chatwin, 1957; Ketchen and Forrester, 1966). By the 1950s the U.S. and Canadian fisheries were experiencing declines in catches that accelerated through the 1970s (Harry, 1959; Pedersen, 1975), reaching minimums around or below 10% of the unexploited levels during the 1980s through the early 2000s (Starr, 2009; Haltuch et al., 2013). In addition to declining catches, biological data collected during 1980-1996 showed a prolonged decline in the proportion of young fish entering the population (Haltuch et al., 2013), likely due largely to heavy exploitation of highly vulnerable spawning aggregations in both the U.S. and Canada. In the early 1990s Canada implemented catch regulations in an attempt to halt the decline in petrale sole abundance and declared no directed fishing since 1996 (Fargo, 2000) and current landings remain low due to petrale bycatch in the trawl fishery. The U.S. fishery continued, sustained by limited increases in abundance due to above average recruitment during the late 1990s that drove a small increase in abundance that peaked in 2005, followed by

declining abundance as strong year classes passed through the fishery (Haltuch et al., 2013). Since 2010, abundance and therefore U.S. fishery catch, has fluctuated in response to a few years with above average recruitment during the late 2000s followed by a lack of incoming recruits, resulting in the fishery depending upon a limited number of year classes to maintain the stock at or near the target stock size (Haltuch et al., 2013; Wetzel, 2019).

Given the transboundary nature of the petrale sole resource, and the fishery dependence upon a limited number of year classes, better understanding the level of connectivity between U.S. and Canadian waters and mechanistic drivers of recruitment success is a high priority. Ketchen and Forrester (1966) suggested that variation in petrale sole year-class strength is correlated with seawater temperatures and geostrophic wind patterns during the pelagic egg and larval stages, specifically suggesting that eggs rise from spawning grounds then sink as they drift to the northwest and inshore due to predominantly southerly winds. Low density seawater along the coast then acts as a barrier to shoreward transport of the eggs, explaining the absence of juveniles in the nearshore. Similarly, Castillo et al. (1993) and Castillo (1995) suggested that density-independent survival of early life stages is low and show that offshore Ekman transportation of eggs and larvae may be an important source of variation in year-class strength. Stock assessments for petrale sole highlight research and data needs that would substantially improve the ability to understand transboundary petrale sole population dynamics, including studies on stock structure and movement, spatial variability in recruitment, and determining mechanisms that lead the occasional strong-year classes that sustain the fishery.

The horizontal-advection bottom-up forcing paradigm, in which large-scale climate forcing drives regional changes in alongshore and cross-shelf ocean transport that directly impact ecosystem functions (e.g., productivity, species composition, spatial connectivity) (Di Lorenzo et al., 2013), provides a mechanistic framework for testing the hypothesis that cross-shelf and alongshore advection are drivers of petrale sole recruitment strength. This paradigm provides mechanistic pathways through which climate variability and change could drive transboundary petrale sole connectivity and recruitment. Petrale sole are an excellent candidate for mechanistic investigations into oceanographic drivers of recruitment strength because 1) the petrale sole data available for the U.S. waters of the CCS are information-rich, due to the large amount of age and length data that spans multiple generations, 2) petrale sole spawn at well known, localized locations during winter, 3) the U.S. stock assessment model, and thus recruitment estimates, is highly stable, and 4) both previous fisheries and oceanographic research suggests clear, untested, mechanisms for oceanographic drivers of petrale sole early life history transport and recruitment (Haltuch et al., 2013). In eastern boundary current systems, such as the CCS, the impacts of large-scale processes on biological dynamics of marine resources can be evaluated through the analysis of the spatial and interannual variability of mesoscale and submesoscale structures (Keister and Strub, 2008; Giddings et al., 2022), such as meanders, filaments and eddies, where for the former is already implemented automatic procedures for its identification and

tracking (Halo et al., 2014). Thus, this study tests two hypotheses regarding oceanographic transport during petrale sole early life history stages. First, that the drift of petrale sole eggs, larvae, and pelagic juveniles during the winter is largely northerly, providing the biological linkage and opportunity for stock mixing between U.S. and Canada. Second, that cross-shelf transport of pelagic petrale sole from deep water spawning grounds shoreward towards settlement areas on the continental shelf results in stronger recruitments than transport offshore away from settlement areas. The above hypotheses are tested by implementing an individual-based model (IBM) coupled with a ROMS hydrodynamic model to test how pelagic cross-shelf and alongshore advection modulates the transport, connectivity, and settlement success of petrale sole.

Methods

IBM model setting

An IBM of larval drift (e.g. Parada et al., 2010; Hinckley et al., 2016; Parada et al., 2016; Gibson et al., 2019; Hinckley et al., 2019; Stockhausen et al., 2019; Daly et al., 2020) was built to explore the petrale sole pelagic connectivity from discrete spawning grounds to potential settlement areas in the CCS. The IBM was developed within a Lagrangian framework (Ichthyop, Lett et al., 2008), where early life dynamics (spawning locations, trajectories, growth rates, mortality) were forced with the ocean circulation from a ROMS hydrodynamic 2-km configuration model from 1988 to 2008. All pelagic stages and mechanisms such as egg development, larval growth, first juvenile stage, natural mortality, and settlement behavior were specified based on existing literature. The IBM model was relatively simple because the Petrale sole early stages are largely unknown, with most of the available literature going

back to studies from the 60s and 70s. The IBM included five pelagic early life stages that span approximately six months (Pearcy et al., 1977): eggs, yolk-sac larvae, post-yolk sac larvae, older larvae and juveniles (Figure 1). Each early life stage was set with its own time span, growth rate, length, depth preference and swimming behavior parameters (Table 1).

Egg stage

The petrale sole IBM was initialized at the egg stage. Females spawn once each year and fecundity varies with fish size, with one large female producing as many as 1.5 million planktonic eggs (Porter, 1964). Eggs are found in deep waters at temperatures of 4 to 10°C and salinities of 25 to 30 ppt, size ranges from 1.2 to 1.3 mm (Best, 1960; Ketchen and Forrester, 1966; Alderdice and Forrester, 1971; Gregory and Jow, 1976; Love, 1996). Egg stage duration ranges from 6 to 14 days (Alderdice and Forrester, 1971; Casillas et al., 1998) with the most favorable conditions for egg incubation and larval growth being 6 to 7°C and 27.5 to 29.5 ppt (Ketchen and Forrester, 1966; Alderdice and Forrester, 1971; Castillo et al., 1995). Eggs rise to the surface between November and April, remaining in surface waters for 6–14 days (Alderdice and Forrester, 1971; Hart, 1973; Casillas et al., 1998). January 01 roughly corresponding with the peak of petrale sole spawning in the CCS (Alderdice and Forrester, 1971) was used as eggs release time. The vertical positioning of eggs in the water column was modeled by the Stokes' law that combines gravitational acceleration, seawater density, seawater viscosity, mixing and turbulence as environmental parameters, and egg density, egg diameter and egg shape as biological parameters (see Ospina-Álvarez et al., 2012 for further details on the implementation of density-diameter-dependent egg buoyancy on Ichthyop). A diameter mode of 1.26 mm (ranged 1.13 to 1.52) was used. The incubation duration

FIGURE 1
Conceptual model of the petrale sole IBM, illustrating the life stages, depth ranges and mechanisms that modulated early life progression. Movement from offshore spawning sites to inshore settlement zones is passive and dependent on advection. Positive buoyancy (B+), neutral buoyancy (B°), negative buoyancy (B-).
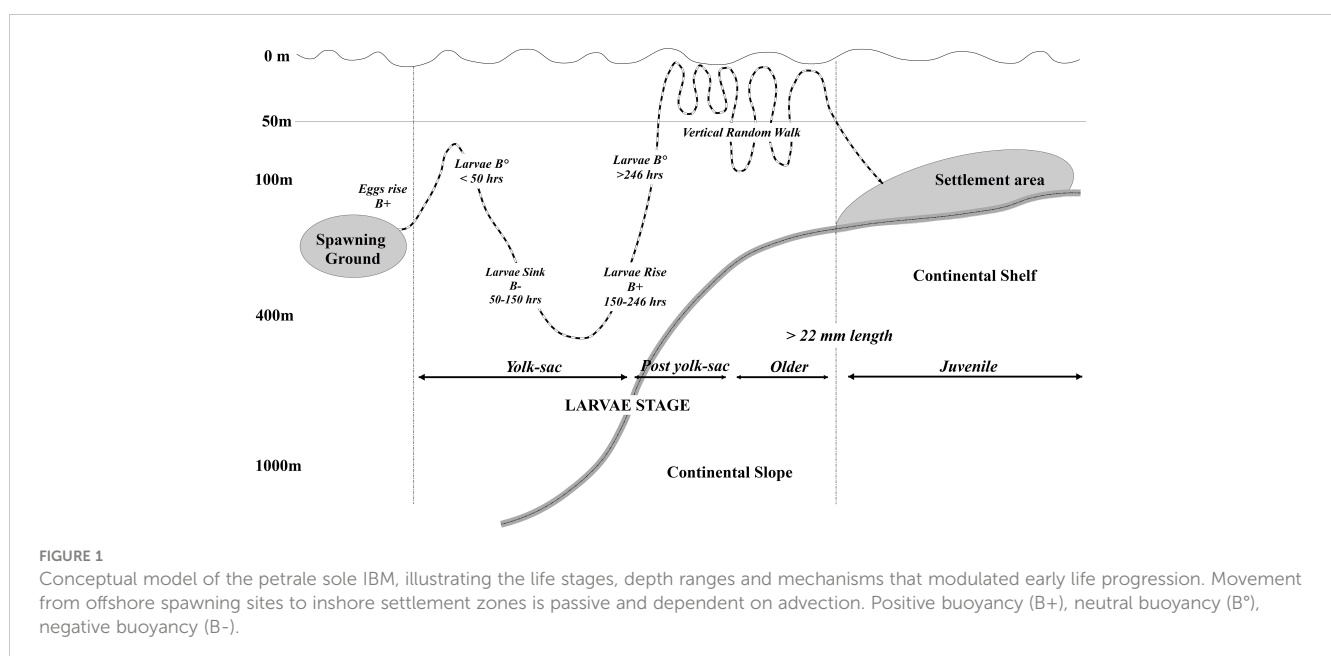
TABLE 1 Early life stages and parameter values used in the petrale sole IBM.

Stage	Parameter	Mode	Range	Units	Source
Eggs	Diameter	1.26	1.13 – 1.52	mm	Alderdice and Forrester, 1971
	Density	1.0249	1.0247 – 1.0262	gr/cm3	Alderdice and Forrester, 1971
	Depth		270 – 460	m	Alderdice and Forrester, 1971
	Incubation time		6 – 13.5	days	Alderdice and Forrester, 1971
	Daily natural mortality	0.15	0.12 – 0.18	days-1	Wetzel, 2019
Yolk-sac larvae	Yolk exhaustion time		10 - 16	days	Alderdice and Forrester, 1971
	Density h<50		Water density	g/cm3	Alderdice and Forrester, 1971
	Density 50 > h < 150		>0.0025% water density	g/cm3	Alderdice and Forrester, 1971
	Density 150 > h < 24650		<0.0025% water density	g/cm3	Alderdice and Forrester, 1971
	Density h > 246		Water density	g/cm3	Alderdice and Forrester, 1971
	Depth		MDL – 475	meters	Alderdice and Forrester, 1971
	Daily natural mortality	0.15	0.12 – 0.18	days-1	Wetzel, 2019
Post yolk larvae	Growth rate	0.105	0.101 – 0.110	mm/day	Pearcy et al., 1977
	Size		5.5 – 12.5	mm	Pearcy et al., 1977
	Vertical swim speed		0.017 – 0.058	cm/s	Pearcy et al., 1977
	Depth		0 – 50	m	Pearcy et al., 1977
	Daily natural mortality		0.12 – 0.18	days-1	Wetzel, 2019
Older larvae	Growth rate		0.101 – 0.110	mm/day	Pearcy et al., 1977
	Size		12.5 – 20.5	mm	Pearcy et al., 1977
	Vertical swim speed		0.017 – 0.058	Cm/s	Pearcy et al., 1977
	Depth		0 – 150	m	Pearcy et al., 1977
	Daily natural mortality		0.12 – 0.18	days-1	Wetzel, 2019
Juvenile	Size		>20.5	mm	Pearcy et al., 1977
	Vertical swim speed		0.017 – 0.058	cm/s	Pearcy et al., 1977
	Depth		10 – 100	m	Pearcy et al., 1977
	Daily natural mortality		0.12 – 0.18	days-1	Wetzel, 2019

(ID, in hours) required for eggs to develop and hatch into yolk-sac larvae was estimated according to a temperature (T) and salinity (Sal) dependent model (Forrester and Alderdice, 1967) where,

$$ID = 482.59 + T*-40.1029 + Sal*-0.23242 \qquad \text{(Eq. 1)}$$

Planktonic petrale sole larvae range in size from approximately 3 to 20 mm, and are found up to 150 km offshore (Moser, 1996; Casillas et al., 1998). The larvae settle at about 22 mm on the inner continental shelf (Pearcy et al., 1977). While there is limited information regarding larval petrale sole vertical migration, other Pleuronectidae species exhibit diel vertical migration, generally within the upper 50 m of the water column, as well as horizontal swimming speeds that increase with larval growth (Verheijen and deGroot, 1966; Hoar and Randall, 1978; Fukuhara, 1988; Grioche et al., 2000; Lanksbury et al., 2007; Baley et al., 2008; Domenici and Kapoor, 2010; Hoffle et al., 2013). According with early life history features three larval stage were considered in our model approach:

Yolk-sac larval stage

After hatching, eggs become yolk-sac larvae. The buoyancy and vertical positioning of yolk-sac larvae were set according to four temporal strata described by Alderdice and Forrester (1971): i) Neutral buoyancy (larvae density equal to water density) between 0 to 50 h, ii) Negative buoyancy (sinking larvae with density > 0.0025% water density) at 50 to 150 h, iii) positive buoyancy (rising larvae with density <0.0025% water density) at 150 to 246 h, iv) Neutral buoyancy (larvae density equal to water density) at >246 h. Yolk-sac larvae have a wide depth range between the mixed layer depth and 475 m. Yolk-sac larvae have no spontaneous movement (Alderdice and Forrester, 1971), therefore neither swimming nor daily vertical migration (DVM) activities were implemented. The yolk-exhaustion time (YE, in hours) required to reach the next stage was estimated through a temperature-dependent yolk-exhaustion model (Forrester and Alderdice, 1967) such that,

$$YE = 923.64 + T * -85.25 \qquad \text{(Eq. 2)}$$

Equations 1 and 2 were calculated using a linear model applied to empirical experimental data from temperature and salinity-dependent incubation time (in hours) for petrale sole eggs and larvae (Alderdice and Forrester, 1971).

Post yolk-sac and older larvae stages

We defined two larval stages after yolk-exhaustion occurs that reflect ontogenetic changes: an early "post-yolk" stage (5.5 to 12.5 mm) vertically distributed between 0 and 50 m, and a "older" larvae stage (12.5 to 20.5 mm) between 0 and 150 m. The total petrale sole pelagic-life duration, including the egg stage, spans approximately 180 d (6 months) with juveniles settling at about 22 mm (Pearcy et al., 1977). However, there is a lack of information on the duration of post yolk and juveniles stages. Given that the combined egg and yolk-sac larvae stages span 22.8 d (range 16 to 29.5 d) (Alderdice and Forrester, 1971) and that the post-yolk larvae (greater than 5.5 mm) to the juvenile stage grows up to 22 mm (180 d), the estimated growth would be 16.5 mm (to reach 22 mm) in approximately 157 d (150 to 164 d). Therefore, the estimated daily growth rate would be 0.105 mm/d (16.5 mm in 157 d), with values ranging between 0.101 and 0.110. From the post-yolk stage spontaneous swimming movements begin (Alderdice and Forrester, 1971), therefore, vertical swimming with random walks were included. The swimming speed for both stages was 0.029 cm/s (range=0.017 to 0.058) (Gibson et al., 2019).

Juvenile stage and settlement

In the waters off British Columbia juveniles are found at 19 to 82 m depth and large juveniles at 25 to 125 m depth (Starr and Fargo, 2004). Juveniles are benthic and found on sandy or sand-mud bottoms (Eschmeyer and Herald, 1983). While no specific areas have been identified as settlement grounds for juvenile petrale sole beyond soft substrate areas on the continental shelf, these settlement areas are spatially distinct from the deep water spawning areas. Once older larvae reached 20.5 mm they were considered as 'juvenile', vertically distributed from 10 to 100 m, with the same vertical random walk and swimming speed of the older larvae.

Juvenile growth rate (JGr, mm/day) was estimated using a temperature-dependent model (Hurst and Abookire, 2006), such that,

$$JGr = 0.0151 + 0.36 \log_{10} * T \qquad \text{(Eq. 3)}$$

Egg, larvae and juvenile mortality was based on an exponential function dependent on the instantaneous daily mortality rate of 0.1 (as used in the las petrale sole stock assessment, Wetzel, 2019). Daily mortality rate was randomly applied each time step following a triangular distribution with +-20%. The superindividuals that make up each particle suffer mortality as they are followed across time and space. This scheme (Scheffer et al., 1995; Megrey and Hinckley, 2001; Bartsch and Coombs, 2004) allowed the use of realistic mortality rates in the IBM by increasing the number of individuals represented by each particle so that a large number of fish in a population can be simulated, assuming that growth, feeding and the probability of mortality of each individual within a superindividual are the same (Hinckley et al., 2016; Parada et al., 2016). We also included mortality to individuals transported outside the study domain.

Inferring petrale sole spawning grounds and egg production

Simulated eggs were released among spatially distinct spawning grounds identified from the winter commercial spawning aggregation fishing locations recorded in the fishery logbook data available from the Pacific Fisheries Information Network (PacFIN) (Table 2). The analysis region was selected to encompass the depth and latitudinal ranges where the petrale sole winter fishery operated across all years. The winter fishery was defined as all trawl tows conducted between November and February, the peak spawning season. Fishery dependent logbook data that included location, trawl catch weights, and trawl tow duration for each trawl tow, from 1981 through 2015 (Pacific Fisheries Information Network) were downloaded and filtered for erroneous records, such as tows whose reported location was on land. Tows whose specified depth was significantly different from the bathymetric depth, derived from the given geographic location, were also removed. All filtered tows with both zero and positive catches within the latitudes where petrale sole spawn were included for analysis.

TABLE 2 Spawning regions and number of particles released per year for the petrale sole IBM model. The number of particles released was based on the proportion of the spawning biomass.

Spawning region	Proportion of spawning biomass	Number of particles
Northern Washington (NW)	0.14	4238
Southern Washington (SW)	0.09	2789
Northern Oregon (NO)	0.31	8920
Southern Oregon (SO)	0.23	6860
Northern California (NC)	0.23	6610
TOTAL	1.0	29417

Logbook data were analyzed by fitting density data into a Vector-Autoregressive spatiotemporal delta-model (VAST; Thorson and Barnett, 2017; Thorson, 2019) following methods similar to those used for U.S. west coast stock assessments (Haltuch et al., 2018; Johnson et al., 2021; Kapur et al., 2021). Both encounter probability and positive catch rates include spatial and spatio-temporal variation. Gamma-distributed errors were used for the positive catch rates within a Poisson-link model (Thorson, 2018). This approach approximates a Tweedie distribution, which has positive mass at zero but is otherwise continuous, however, the Poisson-link model is more computationally efficient. Due to the large amount of logbook data, the spatial variation was approximated using only 300 knots. These knots are distributed on the geographical surface as a function of the spatial intensity of the sampling data and are where spatial processes are estimated by VAST. Catch biomass-per-tow was modeled as a function of the capture year, vessel, and tow location (latitude and longitude). The second-order partial derivatives (Hessian matrix), quantile-quantile (Q-Q) plots, and Pearson residual plots were used to evaluate model convergence and fit. The predictions were plotted against the raw data to check for model misspecification. VAST shows spatial predictions using an extrapolation grid with persistent regions of adjacent grid points through time. Winter petrale sole fishing grounds with consistently high catch rates across all years were identified by selecting the VAST extrapolation grid points with the top 20% of predicted biomass within each year and that were present in at least 14 (40%) of the 35 year time series. These values were chosen after visual inspection across a range of values and were selected to provide distinction between areas of consistently high catch rates that are highly likely to represent spawning areas compared with areas of noticeably lower catch rates that extended shoreward and likely represented migratory routes to and from shallower waters. This focus on regions with consistently high catch rates was to ensure subsequent analyses use regions that are highly likely to represent spawning grounds that agree with traditional winter spawning fishing areas that have remained consistent through time. The extrapolation grid points were then grouped into areas representing core spawning grounds that were consistently occupied through time. Selected extrapolation grid areas were enclosed in polygons using the non-convex hull function in INLA R package (Lindgren and Rue, 2015) and the 'polyclip' R package (Johnson and Baddeley, 2018), with adjacent selected extrapolation grid area groups combined into a single polygon. Using the polygon adjuster function, 'adjustPolygon', in the 'Imap' R package (https://github.com/John-R-Wallace-NOAA/Imap) a limited number of adjacent polygon vertices were manipulated to ensure that each polygon boundary was approximately halfway between the adjacent grid point, each of which was ~1 nautical miles apart. The annual predicted biomass of the extrapolation grid areas within each polygon were aggregated using a weighted average, where the weights were equal to the number of grid points within each extrapolation grid area.

Virtual eggs were released within the spawning ground identified by the analysis above. Egg production in each year was calculated as the sum product of the annual number of females at length, the proportion mature at length (Stawitz et al., 2015), and the fecundity at length (Hannah et al., 2002; Lefebvre et al, 2019). Then egg production in each year was allocated to each spawning area using the proportion of the estimated biomass in each spawning polygon from VAST analysis above (Table 2). The number of eggs is too high (order of millions) to manage individual eggs through computational simulations, thus, a super-individual approach (Scheffer et al., 1995) allowed for each virtual egg to represent a proportion of the estimated egg production in each spawning ground and year. Spawning polygons were aggregated into spawning regions for further analyses using the IBM. A total of 30,000 virtual eggs were released each year, proportionally distributed among spawning regions according to the estimated egg production (Stawitz et al., 2015) in each area and year. An algorithm was used to filter particles that reach model nodes that are considered land (those particles are removed from the simulation ~300). The number of eggs represented by each virtual egg varied across spawning regions and year, capturing the spatio-temporal variation in spawning biomass. In each spawning region virtual eggs were distributed vertically between 270 m to 460 m (347 m on average).

Hydrodynamic model: velocity and eddy patterns

The ocean circulation (vertical and horizontal) and physical properties (temperature and salinity) from a ROMS hydrodynamic 2-km configuration model (NEP, Curchitser et al., 2005; Hermann et al., 2009; Danilson et al., 2011), for the period from 1988 to 2008 was used to study transport and connectivity of the petrale Sole. This period was chosen to encompass a time series with a large range of spawning biomass sizes, from highly depleted to strongly increasing, and a period of inter-annually variable recruitment, while balancing computational time needed to run the IBM. The oceanographic outputs from the ROMS model were validated with physical oceanographic data collected during the NWFSC Pacific hake acoustic survey, including temperature, salinity, and currents, as these data are not used in the ROMs model. With a few exceptions, due to equipment failure or survey conflicts, data was available for survey years during 1992 to 2015. We theoretically explore the impacts of variability in cross-shelf and alongshore transport (e.g. Combes et al., 2013) to potential settlement success. Combes et al. (2013) found that 10 km ROMS models were able to capture both the mean large-scale features of the mesoscale activity, which influences cross-shelf transport, and the subsurface poleward flow in the CCS, which is likely to be important for petrale sole pelagic transport. We used the higher resolution model (2 km) from 1988 to 2008 to capture mesoscale and submesoscale dynamics which potentially impact transport and connectivity of petrale Sole. Interannual and climatological velocities at LS3 (45.9-48.8°N), LS4 (42.4-45.9°N) and LS5 (40.2-42.4°N) sectors (Figure 2)
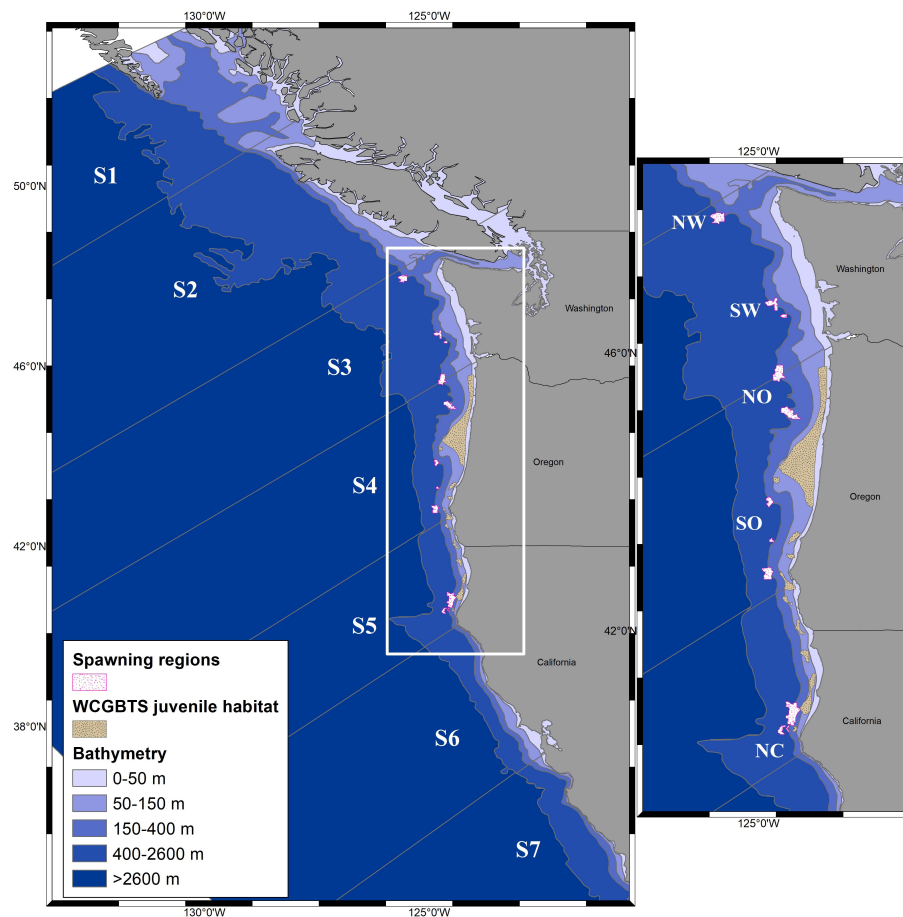
FIGURE 2
California Current System domain divided into seven latitudinal sectors (LS1 to LS7) and five bathymetric strata (left). Zoomed white box shows the five spawning polygons (SPs) and the ten identified WCGBTS settlement area (right).

integrated from the first 100 km (from the coast) were analyzed based on simulated velocities from the ROMS model. In addition, integrated u and v velocity components over time integrated along the latitudinal range were analyzed for the same sectors.

Mesoescale and submesoescale processes was evaluated by detecting and following eddies in order to study possible mechanism that allow simulated particles to be transported or retained in oceanographic structures. Eddy detection was performed on the ROMS model output following the method that combines a physical and a geometric detection method based on Penven et al. (2005) and Halo et al. (2014). For the physical criterion, the algorithm uses the Okubo-Weiss approach (Okubo, 1970; Weiss, 1991) to identify eddies in regions where rotation is considered predominant above the strain rate when Okubo-Weiss $< -2 \times 10-12$ s-2 (Chelton et al., 2007). In addition, to avoid errors associated with the physical criterion (Chelton et al., 2011), an eddy is identified as a closed contour of SSH (Sea Surface Height), where its center is characterized by having a local endpoint of SSH. Eddies were tracked each time step along the whole simulation. The spatio-temporal properties of mesoscale eddies were described in relation to the accumulated number of cyclonic (Nc) and anticyclonic (Na) eddies, and its polarity, defined as the standardized ratio (Na−Nc)/(Na+Nc) within each model cell (Dong et al., 2022).

Connectivity and juvenile settlement success

Connectivity was analyzed considering alongshore and cross-shelf variability. For alongshore analysis the CCS domain was divided into seven latitudinal sectors (LS1 to LS7), each one of relatively similar spatial extent, based on geographic structures such as islands (Moresby, Vancouver), rivers (Washington) and the coastline shape (Mendocino cape). For cross-shelf analysis the CCS was divided longitudinally into five cross-shelf strata based on bathymetric isobaths of 0 to 50 m, 50 to -150 m, 150 to 400 m, 400 to 2600 m, and >2600 m (Figure 2).

The pelagic larval duration ends with successful juveniles settling on the inner continental shelf at 22 mm length (Pearcy et al., 1977). Two potential settlement areas were used to identify a successfully settled 22 mm juvenile: 1) the inner shelf area, defined as the area encompassing both the 0-50 m and 50-150 m bathymetric isobaths, and the 2) 2-year old habitat area (JH), identified according the spatial distribution of 2-year old (≤ 18cm) petrale sole from the West Coast Groundfish Bottom Trawl Survey (WCGBTS) (Keller et al., 2017). While it would be preferable to identify settlement areas for petrale sole using age-0

fish, there are no observations of newly settled age-0 petrale sole in U.S. waters of the California Current and there are very few observations of age-1 petrale sole from the WCGBTS. The inner shelf settlement areas are based on expert knowledge of petrale sole early life history, and represent hypotheses for where age-0 petrale sole are likely to settle.

The WCGBTS data collected from 2003 through 2015 were used to identify juvenile habitat areas using small fish ≤ 18 cm in length. The WCGBTS subsamples each tow for species specific biological data. For each tow, the subsampled weight of small petrale sole ≤ 18 cm was expanded to estimate the total catch weight of petrale sole ≤ 18 cm following methods in Tolimieri et al. (2020). The small petrale sole catch rate for each tow (CPUE) was calculated as the estimated total catch weight in each tow over the trawl area swept. Next, the same VAST modeling tool applied to the spawning ground fishery data was fitted using the WCGBTS small petrale sole CPUE as the response variable. Both encounter probability and positive catch rates include spatial and spatio-temporal variation. Gamma-distributed errors were used for the positive catch rates within a Poisson-link model (Thorson, 2018). The predictor variables were year, vessel, tow location (latitude and longitude) and depth. Depth was assigned to each knot using a bathymetric depth function in the Imap R package (https://github.com/John-R-Wallace-NOAA/Imapa). Spatial variation was approximated using 600 knots in the VAST model. The second-order partial derivatives (Hessian matrix), quantile-quantile (Q-Q) plots, and Pearson residual plots were used to evaluate model convergence and fit. The predictions were plotted against the raw data to check for model misspecification. Juvenile habitat area was identified by selecting the VAST extrapolation grid points with the top 15% of predicted CPUE within each year and that were present in at least 3 (23%) of the 13 year time series. Polygons were created using the same methods implemented for the fishery logbook data, with the exception of a few juvenile habitat polygons that were slightly expanded to include observations near the extrapolation grid area groups but that were not selected as a top area with the criteria used.

Results

Spawning grounds and juvenile habitats

Spawning grounds and juvenile habitat areas from their respective VAST models fit well. In both cases positive definite Hessian matrices indicated the model converged and Q-Q plots followed a 1:1 relationship indicating good fit to the data (Figure S1). Pearson residual plots across space and time did not show spatial and spatiotemporal patterns suggesting good model fit.

Eleven spawning grounds that range from 40.5° to 48.0° latitude were selected based on the methods criteria. The average minimum depth across all areas was 227.3 meters (CV = 0.50) and the average maximum depth was 677.3 meters (CV = 0.24). Spawning grounds ranged from 17.6 to 400.3 square kilometers in size with an average of 145.2 square kilometers (CV = 0.80). The largest spawning ground ranges from 40.6° to 40.9° latitude and along with two

other small areas encompasses a cluster that contains the most southerly areas. An example containing two of the winter spawning areas from northern Oregon is shown in Figure S2. On the mid to upper right of the top polygon in Figure S2 note that if the use of a greater number of knots was possible those points may not have been included as part of the polygon. The 35 years of logbook fishery data restricted VAST to 300 knots which is half of the 600 knots that was used for the 13 years of WCGBTS survey data. For the lower polygon in Figure S2 there are points of the second to highest level just to the right of the bottom right points within the polygon. For clarity those are not shown in this figure, but when seen in a figure that shows all points they visually support those points belonging to the highest category and hence being included within the polygon.

Nine out of the eleven spawning grounds have increasing biomass trends over the study period, with the fifth spawning area counting north to south (latitude centroid = 45.13°) showing the largest increase of ~300% during the last five years of the study (Figure 3). Spawning grounds three, seven, and eleven, counting from north to south, were relatively small and contributed the lowest levels of biomass across the study period. These spawning grounds are sparsely distributed along the coast with a small amount of clustering. However, in order to facilitate subsequent interpretation and connectivity analysis, these were grouped geographically into five spawning regions: northern Washington, southern Washington, northern Oregon, southern Oregon and northern California (Figure 2).

Ten potential settlement areas were identified from the 2-year old WCGBTS data. These areas are regularly distributed within the latitude range of 40.5° to 45.7°. The average minimum depth over the areas was 58.3 meters (CV = 0.27) and the average maximum depth was 114.1 meters (CV = 0.21). The size of the areas ranged from 30.5 to 3562.7 square kilometers with an average of 468.1 square meters (CV = 2.33). The largest and most northerly area is ~3 times larger than the sum of the other nine areas combined. The bulk of this large area extends from 44.1° to 44.7° latitude, but it extends further along the coast to both the north and south (Figure 2).

Transport and connectivity pattern

The location of the spawning source, the year, the dominant circulation pattern and the drift time all had an impact on transport and connectivity. On average, a relatively clear along-shelf transport of the pelagic stages was observed, especially for juveniles from spawning regions off northern Washington and southern Washington, which were transported to Moresby (LS1) and Vancouver Island (LS2), Canada. Juveniles released NO were transported moderately northward to Vancouver Island (LS2), Canada and Washington (LS3), and were also retained off Oregon (LS4). Individuals from southern Oregon and northern California were mostly retained off Oregon and California (LS5), with no individuals located north of Vancouver Island. High interannual variability was observed, with highest negative connectivity anomalies for juveniles from northern Washington in 1988, and
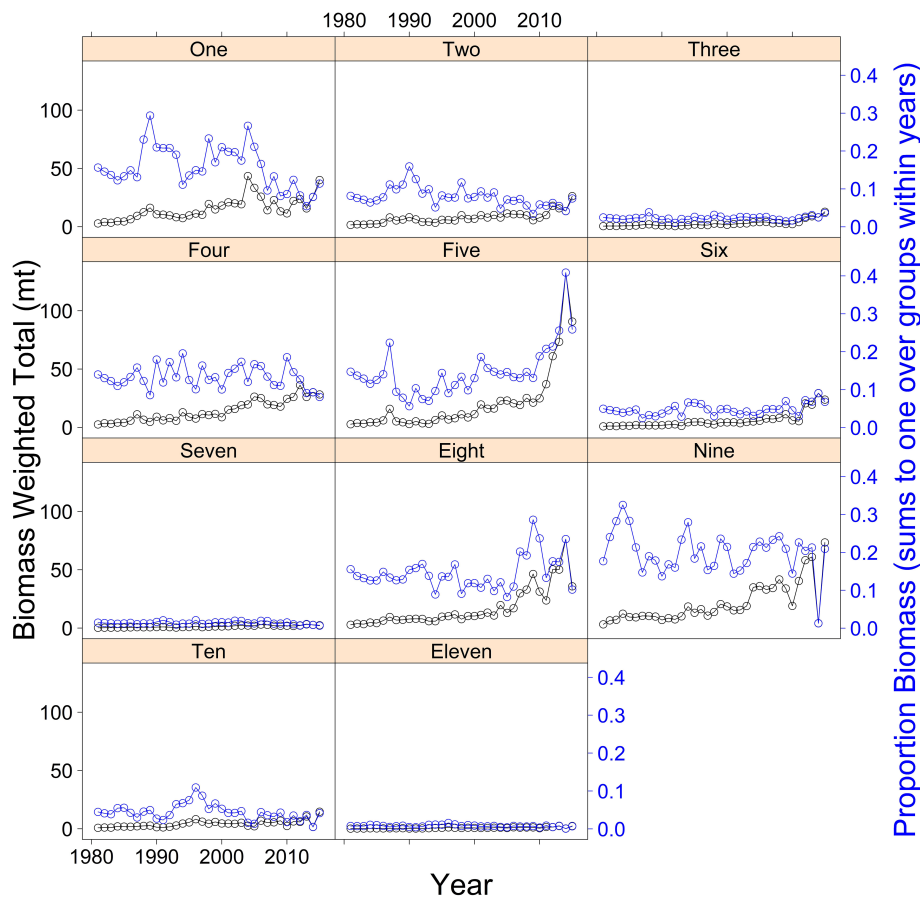
FIGURE 3
Petrale sole spawning biomass weighted total (metric tons) by year (black) and proportions of biomass summed to one over groups within years (blue) for the eleven selected spawning ground groupings.

northern Oregon in 1988, 1989, 2002, 2003, 2004 and 2008. Conversely, highest positive connectivity anomalies were observed for the northern Washington and northern Oregon areas in 1989 and 2005, respectively (Figure 4).

Settlement success and trajectories

The number of successful individuals showed large interannual variability, with a minimum of 1.05×10^8 in 2002 and a maximum of $3,77 \times 10^8$ in 2005 (average: 1.95×10^8 juveniles, SD = 6.32×10^7) (Figure 5A). Between 4.1% (2002) and 19.0% (1993) of annual released individuals were successfully settled in the inner shelf area, and between 0.15% (1999) and 0.70% (1990) were settled in the 2-year WCGBT settlement area (located off Oregon) (Figure 5B).

The spatial distribution of successful individuals among the latitudinal sectors remained relatively consistent through time, where trajectories were modulated by current direction and intensity, and through the formation of mesoscale oceanographic structures (Figure 6A). In particular, Moresby Island (LS1 - Queen Charlotte Sound) received 17.2% of the successful individuals (SD = 6.6%), strongly provisioned by a northward coastal pathway from

the northern Washington spawning region (Figures 5A, 6B). Also northward, Vancouver Island (LS2) received a larger proportion of successful individuals, 32.6% (SD = 6.6%, Figure 5A), mostly from the southern Washington spawning region (Figure 6D). The Washington (LS3) and Oregon (LS4) sectors received 19.1% (SD = 4.3%) and 18.4% (SD = 5.7%), respectively (Figure 5A), were less influenced by the northward transport, and were retained close to the northern Oregon and southern Oregon spawning regions, reaching no further north than Vancouver Island (Figures 6F, H). North California (LS5), Central California (LS6) and South California (LS7) showed a lower percentage of successful individuals, 8.4% (SD = 4.0%), 3.9% (SD = 3.6%), and 0.5% (SD = 0.5%), respectively (Figure 5A), being largely transported shoreward and in a northerly direction to the Oregon coast from the northern California spawning region (Figures 6F, H, J). It was also noted that there was strong juvenile loss because offshore transport through many westward pathways. Individuals from the northern Washington and southern Washington spawning regions were transported northward and westward to offshore waters north of Vancouver Island (Figures 6C, E), while individuals from the northern Oregon, southern Oregon and northern California spawning regions were exported directly westward (Figures 6G, I, K).
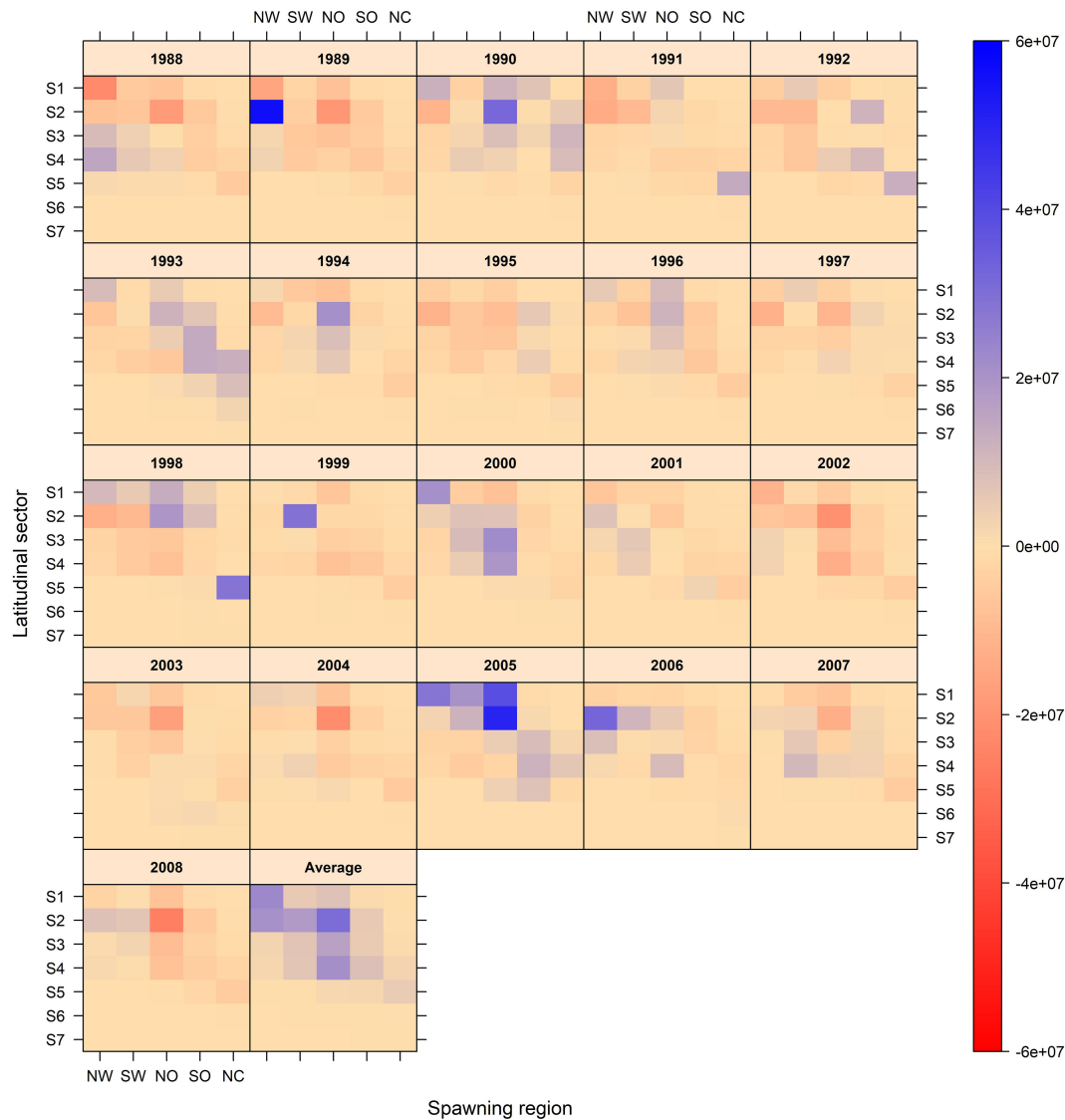
FIGURE 4
Interannual variability of successful individuals connectivity from spawning regions to latitudinal sectors. The last plot is the average for the entire period 1988 to 2008.

Flow patterns in the coastal CCS

Analysis of the interannual variability of the pattern of current flow at three latitudinal sectors located at LS3, LS4 and LS5 integrated for the first 100 km from the coast showed that the LS3 sector had a north-northwest current flow annually during January to March with a current fluctuation toward S-SE during April-June. These repeating annual patterns favor northward transport and retention toward the coast (Figure 7A upper). At LS4 and LS5 the flow pattern integrated 100 km from the coast, showed a NE flow early in the year and a strong current flow in the SE direction until June-July each year, favoring export offshore (Figure 7A, middle and lower). The exports were stronger in 1998 and 1999. The climatology of the currents at these sectors showed a clear pattern where the LS3 sector showed on average a very strong

north-northwest flow during January to March with a current fluctuation toward S-SE during April to July (Figure 7B upper). LS4 and LS5 sectors showed a common flow pattern (LS5 more intense) with a NE flow from January to March and a strong current flow in the SE direction during April to June, favoring export offshore (Figure 7B, middle and lower). This pattern of export is stronger at LS5. Integrated velocities along the first 100 km through the latitudinal range showed a velocity gradient from the north to south sectors (Figures 7C, D). Velocity components integrated the first 100 km at different latitudes, showed a predominant flow N and E, while LS4 and LS5 showed a predominant flow N and W (Figures 7C, D). From these results we can infer the difference in conditions at LS3, LS4 and LS5, while LS3 sector precludes retention towards the coast during April to June, LS4 and LS5 offshore losses intensified at LS5.
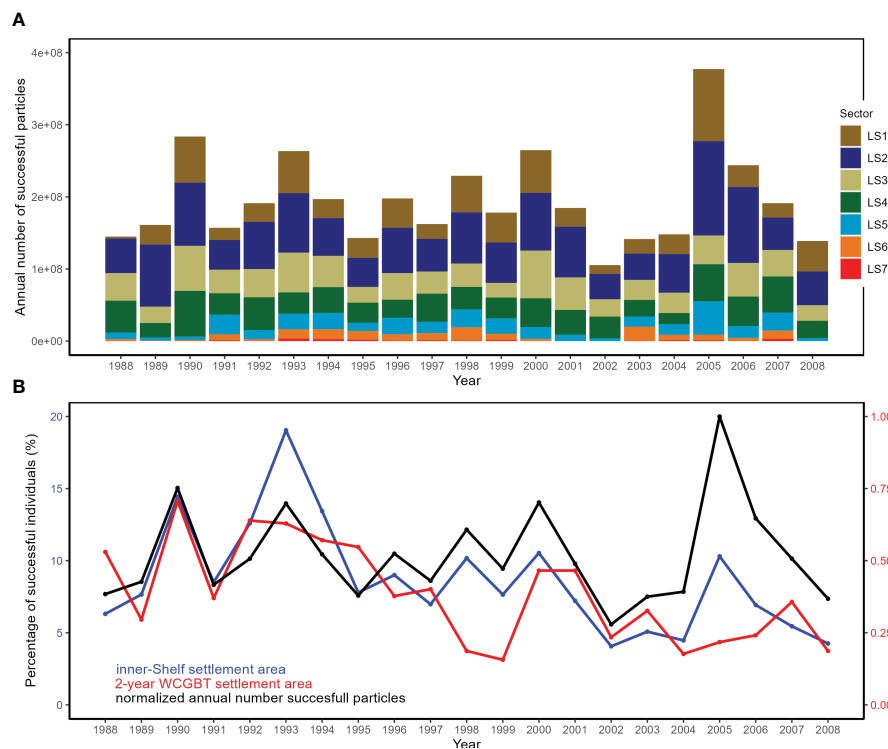
FIGURE 5

(A) Annual number of successful particles among the seven latitudinal sectors between 1988 and 2008. **(B)** Percentage of successful individuals settled each year within the inner shelf area (blue) and 2-year old settlement area from the WCGBT fishery data (red), and the normalized annual number of successful particles (black).

Mesoscale forcing and larval trajectories

The generation, development and transport of mesoscale eddies is a feature of the entire coastal fringe off the west coast of North America (Figure 8A). On average, a rather homogeneous cumulative pattern of eddies occurs in the first ~300 km from the coast from 1988 to 2008 (Figure 8A). The average distribution and density of eddies differs between the LS3 (north of 45.9°N) and LS5 (south of 45.9°N) sectors. The polarity field of the eddy distribution, on average, shows a greater predominance of anticyclonic eddies across the study area (Figure 8B). The LS5 sector has the highest density of anticyclonic eddies, with decreasing density towards higher latitudes (Figure 8B). In the LS3 sector, a coastal band of negative polarity characterizes a prefuse cyclonic eddy activity.
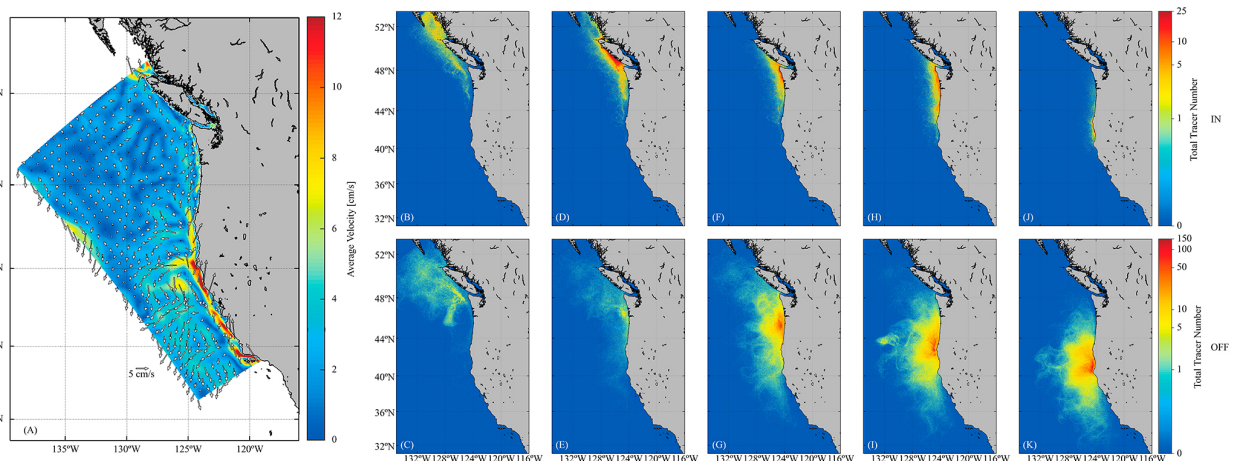
FIGURE 6

(A) Average current velocity, direction and intensity. Trajectories of successful (top) and unsuccessful (bottom) individuals released by area; **(B, C)** northern Washington, **(D, E)** southern Washington, **(F, G)** northern Oregon, **(H, I)** southern Oregon and **(J, K)** northern California.
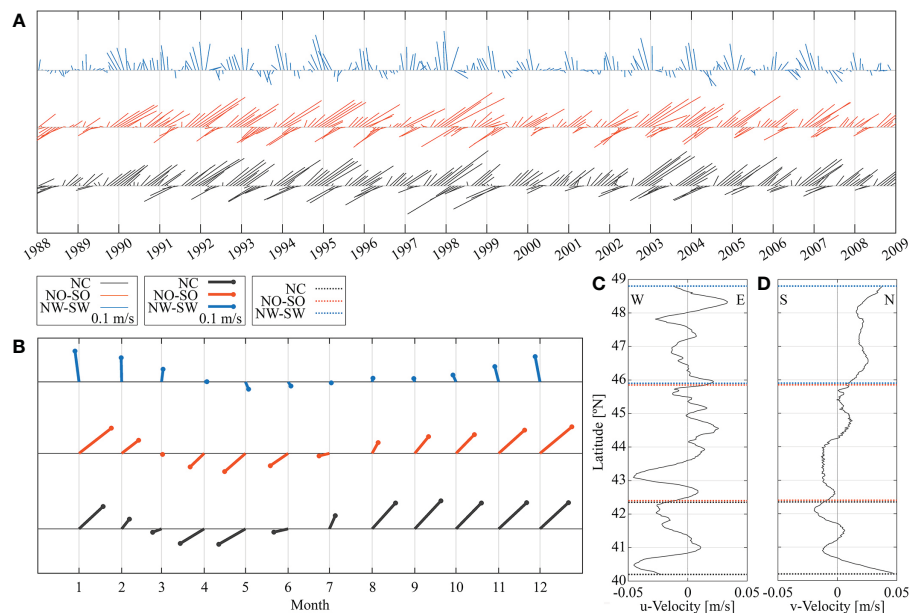
FIGURE 7

(A) Stick-plot diagram of interannual velocities and direction of the current as simulated by the ROMS model generated at northern Washington-southern Washington, northern Oregon-southern Oregon and northern California sectors. **(B)** Stick-plot diagram of climatological current velocities and direction of the simulated current at northern Washington-southern Washington, northern Oregon-southern Oregon and northern California sectors. **(C)** Integrated u and **(D)** v velocity components over time along the latitudinal range between the coast and 100 km.

Here, the cyclonic eddies marked in blue showed trajectories that are retained at the first 100km (102 eddies), with relatively low losses of cyclonic eddies offshore (39 eddies, black trajectory lines, Figure 8C). In LS5, a relatively low amount of cyclonic eddies are retained at the first 100 km (~40) and most of the cyclonic eddies propagate offshore (158 eddies, black trajectory lines, Figure 8C). Few anticyclonic eddies (Figure 8D) stayed inside 100 km in LS3 (36 eddies, marked in red) and relatively low amount of losses offshore (14, black lines). In LS5 only 18 anticyclonic eddies are retained, while most of them propagate offshore (223 eddies, Figure 8D). Thus, the coastal band of 100 km in the LS3 sector tends to retain eddies and therefore successfull larvae within the inner shelf settlement area, while the LS5 sector eddy activity has most of the eddies trajectories toward offshore regions exporting unsuccessful larvae.

Discussion

This study contributes to understanding petrale sole spawning grounds that have been consistently occupied across a range of stock sizes, regions of successful juvenile settlement, and clearly identifies transboundary connections and driving mechanisms between spawning and prospective settlement regions. These well known discrete spawning areas have been exploited by the fishery from the 1960s forward (Haltuch et al., 2013), with commercial logbook data being the only available data source documenting these areas in recent decades. The most recent 2019 assessment estimates showed the minimum spawning biomass around 2,000 metric tons in 1992-1994, followed by a gradual increase through

the study period, with the years 2004 to 2008 exceeding 4,000 metric tons (Wetzel, 2019). Petrale sole spawning biomass was last estimated to be around or above 4,000 metric tons during the 1970s.

Prospective juvenile settlement regions from 2-year-old WCGBTS data are quantified and evaluated as age-0 settlement regions for the first time. There is an unmodeled period between settlement at 6 months and 2 years (known as the post-settlement searching phase, Cooper et al., 2013), where benthic dispersal mechanisms remain unknown. WCGBTS settlement areas identified from the survey data are limited due to the small number of age-2 fish sampled, and the lack of observations for newly settled age-0 or age-1 petrale sole. The fishery does not serve as a data source for juvenile petrale sole due to selection of fish beginning about age-4. Additionally, near-shore opportunistic samples from other research programs do not collect petrale sole (pers comm J. Field and W. Wakefield). While all available data sources that may inform juvenile habitat in US waters have been investigated, results suggests that the settlement areas inferred from the survey are not realistic due to the low number of successful settlers in these regions. Survey data collections of age-2 petrale sole are likely taking place after dispersal from settlement areas. Thus the depth zones used to specify settlement regions remain the best option for understanding where along the west coast of North America petrale sole settle to benthic nursery habitats.

This is the first ROMS coupled IBM for petrale sole in the CCS, and provides insight into the interconnectedness of petrale sole pelagic life stages, from distinct deep-water spawning regions to inshore settlement zones. The IBM design specifically employed environmental variables to represent the growth of life stages while also reflecting existing early life history knowledge, including early
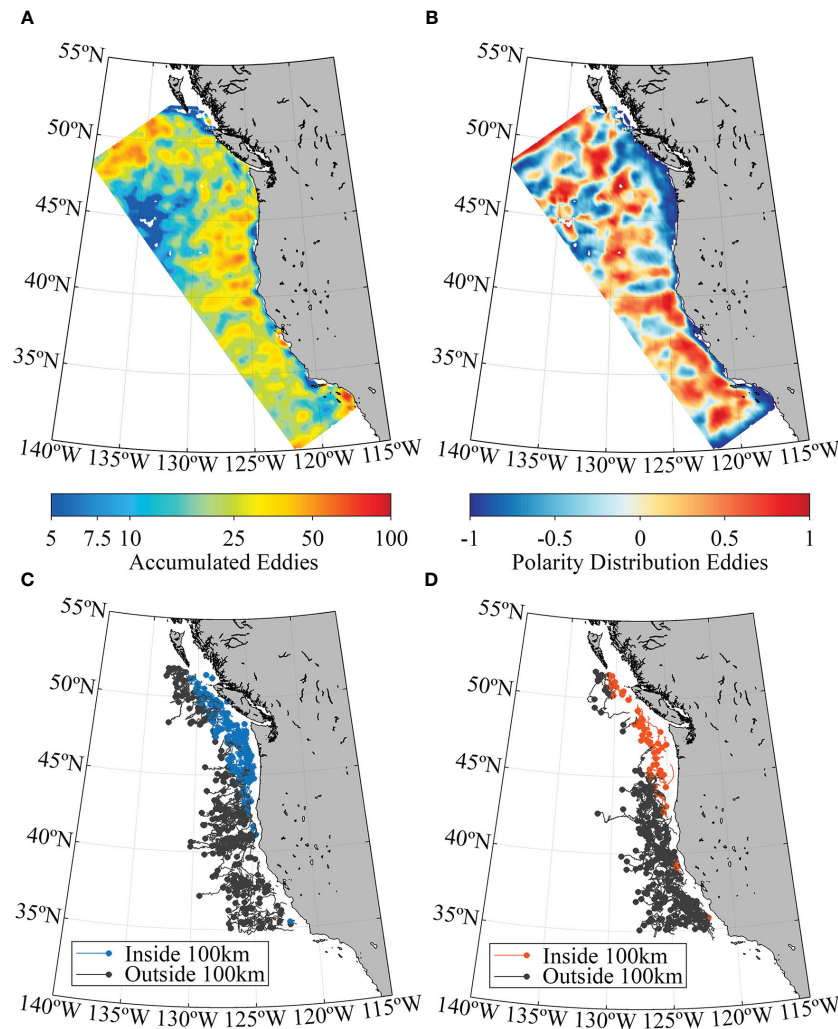
FIGURE 8
(A) Average accumulation of mesoscale eddies, **(B)** average spatial distribution of eddy polarity, **(C)** trajectory of cyclonic eddies, in blue the ones that originated and stayed within the first 100 km from shore and **(D)** trajectory of anticyclonic eddies, in red the ones that originated and stayed within the first 100 km from shore. Eddies in black are those whose trajectories end up beyond 100 km offshore from the coast. Eddy estimates span the period 1988-2008, in 1/4° domains, based on the daily outputs of NEP5 with 1/10° resolution.

stages (eggs, larvae, and juveniles), depth ranges, and sizes. Previous applications of ROMs coupled IBMs to flatfish species have allowed a better understanding of dispersal mechanisms and their impacts on larval connectivity, as well as explorations of how interannual regional oceanographic variability may impact settlement and subsequent recruitment success (Sadorus et al., 2020). A common reproductive strategy among flatfish species appears to be the coupling of the spawning activity with oceanographic dynamics that increase the probability of access to settlement habitats (Goldstein et al., 2020), but this strategy may vary according to the duration of the larval period, spawning season and the coastal proximity of spawning localities to the coast. Spring spawning species that utilize nearshore spawning areas and exhibit short larval duration probably have comparatively lower dependence on current dynamics. However, winter spawning species that utilize deep offshore spawning locations tend to have longer larval durations and stronger dependence on oceanic connectivity to

transport larvae to remote settlement areas (Barbut et al., 2019). The former strategy is particularly sensitive to the expected environmental modifications associated with climate change. For example, it has been predicted that due to the increase in temperature, the common sole (Solea solea) spawning in the English channel will spawn earlier, resulting in increased larval duration time and distance traveled that may cause increasing recruitment (Lacroix et al., 2017). However, increased successful transport associated with increasing temperature and changes in predominant currents, may activate density-dependent processes that negatively impact recruitment success, as has been observed in North Sea plaice (Pleuronectes platessa) (Hufnagl et al., 2013). Petrale sole have a long larval duration, with up to 6 months of pelagic life, and larval transport that is strongly dependent on hydrodynamics. Our results suggest that mesoscale and submesoscale structures are key for the successful settlement of petrale sole. Despite the offshore transport of a large proportion of

larvae, many successfully arrive at inshore settlement areas due to eddies retained within the first 100km of the coast (Figures 8C, D) that retain larvae nearshore during northward transport.

This study unequivocally demonstrates that petrale sole is a transboundary stock shared between the U.S. and Canada and supports the significance of the Canadian waters as nursery grounds, as previously suggested by Ketchen and Forrester (1966). Simulations showed a clear trend of northward transport from deep water spawning zones on the continental slope off Washington and Oregon towards inshore settlement areas off Vancouver and Moresby Islands, with some interannual fluctuation. Petrale sole is currently assessed and managed independently by the U.S. and Canada. However this work suggests a need for transboundary scientific cooperation to inform regional fishery managers. Fisheries policy naturally depends on a clear description of management boundaries that determine the geographic area in which stocks are evaluated and rules are put into effect (Kerr et al., 2017; Ramesh et al., 2019). A potential divergence with the underlying, dynamic population structure results from the fact that management boundaries are frequently rigid and established by politically agreed-upon or historically recognized population units (Berger et al., 2021). A further consequence of disregarding complex population structure and stock connectedness is a misunderstanding of the level of fish productivity, which can result in less-than-ideal fisheries management (Kerr et al., 2017). Overexploitation of special spawning components is the main ecological worry since it has the potential to destroy biodiversity, impair productivity, and destabilize local and regional stock dynamics. Spatially explicit models, and dynamic management options that help align management and population boundaries would likely reduce estimation biases and management risk, as would closely coordinated management that functions across population boundaries (Berger et al., 2021).

Physical dynamic simulation and horizontal transport

The circulation model presents realistic horizontal transport that has been previously validated (e.g., Politikos et al., 2018; Dussin et al., 2019). Frequent strong coastal eddies characterize the CCS, an eastern boundary upwelling system. On average, a rather homogeneous cumulative pattern of eddies occurs within ~300 km of the coast, over the study years (1988-2008). The polarity of the eddy distribution shows a predominance of anticyclonic eddies over the study area, a typical trend for eddies in eastern boundary systems (Chelton et al., 2011). The average distribution and density of eddies differs between the northern and the southern regions. In the southern region, the number of eddies was low and rather homogeneously distributed and characterized by mainly anticyclonic eddies. The core of low concentration of eddies is located precisely in the separation zone of the North Pacific Subarctic Current (Hickey and Royer, 2001), which is related to

low mesoscale activity (Cheng et al., 2014). A larger number of cyclonic eddies are present in the northern region, a distribution attributable to the hydrodynamic processes of the CCS (Marchesiello et al., 2003; Capet et al., 2008; Seo et al., 2015). Cyclonic eddies influence the retention and dispersal of reproductive products along the California coast. Most simulated particles exhibited complex individual trajectories during the model runs, suggesting a strong influence of submesoscale (~10km) and mesoscale eddies (~200km). These eddies help upwelled water with increased biological activity travel intensely and over a long distance across the shelf (Chenillat et al., 2018). Specifically, mesoscale and submesoscale eddies play an important role in retention, advection offshore, transport and connectivity to the north of 46°N. The reproductive activity associated with the petrale sole spawning regions located off Washington (42-46°N) are affected by this dynamic. While the development of coastal cyclonic eddies off Washington favors retention, coastal cyclonic eddies off south Oregon and north California (35-42°N) are characterized by movement in a southwesterly direction away from the coast, potentially resulting in fewer successful settled juvenile petrale sole.

Study caveats and future refinements

We built a comprehensive IBM for the early life stages of petrale sole using all available biological data, including growth processes, movement, and mortality. However, future IBMs should explore additional processes to improve the mechanisms embedded in the model, further specify connectivity and settlement, and ultimately increase the understanding of the recruitment of petrale sole in the CCS domain (Haltuch et al., 2020). Some of these mechanisms include spawning-related elements such as batch fecundity, timing and frequency, as well as summer and fall ocean dynamics prior to spawning (May to October) that are important for female preconditioning and subsequent year class strength. The addition of oxygen, and impacts of hypoxia, could be particularly important for spawner preconditioning given increasing levels and spatial extent of hypoxia in the CCS. Research on rockfishes and sablefish has also shown that female condition may influence whether or not an individual spawns, the quality and number of eggs, and subsequent year class strength (Sogard et al., 2008; Rodgveller et al., 2016; Tolimieri et al., 2018). Female condition is not considered in this study, although it may result in time variation in fecundity or egg quality, and provide an indicator of year class strength for petrale sole (Haltuch et al., 2020). Understanding the impact of marine heat waves that drive upwelling habitat compression of cool waters towards the coast during anomalously warm years could also be important for the pelagic life stages of petrale sole given the demonstrated ability of marine heat waves to alter pelagic species distributions (Santora et al., 2020; Schroeder et al., 2021). In addition, larval feeding strategies such as first feeding and movement-bioenergetics coupling, where both biogeochemical components and prey availability can impact the energy cost of searching for food, are important considerations that

can impact larval growth (Politikos et al., 2015; Parada et al., 2016; Boyd et al., 2020) and could be an important aspects to address. The complexity of the IBM model could be expanded by parameterizing these key processes that fully account for the functional connectivity of species (Gregory Lough et al., 2017), however, this also requires a robust body of data not yet available for the petrale sole.

Spatial refinements to regions identified as both spawning grounds and juvenile settlement regions would improve this study. While fishery catches from spawning areas identified in this study include larger, mature individuals and have limited bycatch of non-target species, there are few visual confirmations of spawning locations. Spawning grounds recognized in this investigation could be refined using visual survey methods to better determine the spatial extent of areas with fish demonstrating pre-spawning or active spawning behaviors (e.g. Powell et al., 2022). Given that specific settlement areas for juvenile petrale sole remain elusive, this study evaluated one alternative hypothesis regarding settlement depths, from 50 to 150 m depth, that began to provide insight into where to find petrale sole early life stages between spawning and survey observations. Future field work could be guided by the regions identified as settlement areas for age-0 petrale sole in the IBM results. It would be valuable to be able to better quantify the essential fish habitat (PFMC, 2019) for newly settled age-0 petrale sole given the high commercial importance of this fish stock and the current lack of data for age-0 and age-1 fish.

Our study clearly shows that petrale sole off the west coast of North America are a transboundary stock with important settlement areas off the coast of British Columbia, thus expansion of this study into Canadian waters is particularly relevant. Future enhancements to this study should include expanding the spawning grounds and virtual egg releases into Canadian waters, potentially using settlement polygons different from the ones inferred in this study off the coast of Vancouver Island (Ketchen and Forrester, 1966) and spatially extending the current IBM. Incidentally, the estimated spawning biomass of petrale sole has exceeded 10,000 metric tons from 2014 to present (Wetzel, 2019), spawning stock sizes that have rarely been estimated, which provides further incentive to extend the IBM forward in time.

This study illustrates a key mechanism between shoreward and northerly transport of petrale sole pelagic life stages by cyclonic eddies in the northern California Current system and subsequent recruitment success. An eddy index derived from satellite data could provide a source of operationally available observations upon which to base an eddy index (Chelton et al., 2011; Kurian et al., 2011) for predicting petrale sole recruitment to the survey up to three years into the future. Developing a recruitment index based upon operationally collected observational data from satellites could bypass the current lack of ecosystem wide operational ocean model outputs. Currently available oceanographic model outputs that could be appropriate for creating an annual eddy index are of limited usefulness for operational recruitment predictions in the

northern California Current due to spatial limitations, models do not span the U.S. – Canadian border, and are academic research products dependent upon uncertain funding. The current climate-recruitment relationship for petrale sole is dependent upon such a model (Haltuch et al., 2020).

Oceanographic modeling products could support long-term decadal scale projections of stock productivity given climate change that could be useful for strategic questions of interest to fishers and fishery managers. The clear linkages between petrale sole recruitment and cyclonic eddies could serve as the basis for climate driven projections of future recruitment that can be used to identify how petrale sole productivity may shift due to climate change impacts. Ideally, this would require the development of an eddy resolving coastal model for the California Current that spans the U.S. –Canadian border.

The insights provided by this research set the stage for assessing how climate driven changes in stock productivity, the distribution of pelagic life stages, and connectivity between spawning grounds may be mitigated to achieve climate ready fisheries for the transboundary petrale sole stock. Moreover, combining data from operational models and physical oceanographic observing systems should help fisheries management and create new options for dynamic spatial management and the creation of short-term projections (Hidalgo et al., 2019). Incorporating climate responsiveness into operational short-term recruitment prediction is important for understanding the near term future of the stock and for climate informed tactical fishery decision-making (Sumaila et al., 2011; Miller et al., 2018).

Data availability statement

The raw data supporting the conclusions of this article will be made available by the authors, without undue reservation.

Author contributions

FS, CP and MH were responsible for study conceptualization and biophysical modelling. JW contributed to the spatial analyses of fishery data. SC-G and EC contributed to the analysis of IBM results, and EC developed the ROMs model. The authors interpreted the data and wrote the manuscript together. All authors contributed to the article and approved the submitted version.

Funding

Acknowledgments

We thank Vladlena Gertseva, Owen Hamel, and the two journal reviewers who provided comments that improved this manuscript.

Conflict of interest

The authors declare that the research was conducted in the absence of any commercial or financial relationships that could be construed as a potential conflict of interest.

Publisher's note

All claims expressed in this article are solely those of the authors and do not necessarily represent those of their affiliated organizations, or those of the publisher, the editors and the reviewers. Any product that may be evaluated in this article, or claim that may be made by its manufacturer, is not guaranteed or endorsed by the publisher.

Supplementary material

The Supplementary Material for this article can be found online at: https://www.frontiersin.org/articles/10.3389/fmars.2023.1155227/full#supplementary-material

SUPPLEMENTARY FIGURE 1
Q-Q plots from the VAST fit to the commercial fishery logbook data used to identify spawning grounds (left panel), and the WCGBTS small petrale sole CPUE data used to define juvenile habitat (right panel).

SUPPLEMENTARY FIGURE 2
An example of spawning grounds identified using the VAST extrapolation grid point collections that were included in the top 20% of predicted biomass within each year, and were present in at least 14 (40%) of the 35 year time series. The grid points are shown in red. However, for clarity, the grid point collections are not separately identified in the figure. Adjacent grid point collections were enclosed in a single polygon (thick black lines). The underlying raw data for all years is shown with bubble plots (blue circles). Since time is not represented in the raw data shown, a cluster of points that occurred only over a few years may appear dense but would not meet the criteria.

References

Alderdice, D. F., and Forrester, C. R. (1971). Effects of salinity and temperature on embryonic development of the petrale sole (Eopsetta jordani). *J. Fish Res. Board Can.* 28, 727–744. doi: 10.1139/f71-101

Alverson, D., and Chatwin, B. (1957). Results from tagging experiments on a spawning stock of petrale sole, eopsetta jordani (Lockington). *J. Fish Res.* 14 (6), 953–974. doi: 10.1139/f57-042

Baley, K. M., Abookire, A. A., and Duffy-Anderson, J. T. (2008). Ocean transport paths for the early life history stages of offshore-spawning flatfishes: a case study in the gulf of Alaska. *Fish Fish (Oxf)*. 9, 44–66. doi: 10.1111/j.1467-2979.2007.00268.x

Barbut, L., Groot Crego, C., Delerue-Ricard, S., Vandamme, S., Volckaert, F. A. M., and Lacroix, G. (2019). How larval traits of six flatfish species impact connectivity. *Limnol. Oceanogr.* 64, 1150–1171. doi: 10.1002/lno.11104

Bartsch, J., and Coombs, S. H. (2004). An individual-based model of the early life history of mackerel (Scomber scombrus) in the eastern north Atlantic, simulating transport, growth and mortality. *Fish Ocean.* 13 (6), 365–379. doi: 10.1111/j.1365-2419.2004.00305.x

Berger, A. M., Deroba, J. J., Bosley, K. M., Goethel, D. R., Langseth, B. J., Schueller, A. M., et al. (2021). Incoherent dimensionality in fisheries management: consequences of misaligned stock assessment and population boundaries. *ICES J. Mar. Sci.* 78 (1), 155–171. doi: 10.1093/icesjms/fsaa203

Best, E. A. (1960). "Petrale sole," in *California Ocean fisheries resources to the year 1960* (California Department of Fish and Game), 58–60.

Boyd, R. J., Sibly, R., Hyder, K., Walker, N., Thorpe, R., and Roy, S. (2020). Simulating the summer feeding distribution of northeast Atlantic mackerel with a mechanistic individual-based model. *Prog. Oceanogr.* 183, 102299. doi: 10.1016/j.pocean.2020.102299

Campana, S. (2016). Transboundary movements, unmonitored fishing mortality, and ineffective international fisheries management pose risks for pelagic sharks in the Northwest Atlantic. *Can. J. Fish Aquat Sci.* 73 (10). doi: 10.1139/cjfas-2015-0502

Capet, X., Colas, F., Mcwilliams, J. C., Penven, P., and Marchesiello, P. (2008). Eddies in eastern boundary subtropical upwelling systems. *Ocean Modeling an Eddying Regime* 177, 350. doi: 10.1029/177GM10

Casillas, E., Crockett, L., deReynier, L., Glock, J., Helvey, M., Meyer, B., et al. (1998). *Essential fish habitat West coast groundfish appendix* (Seattle, Washington: National Marine Fisheries Service). Available at: http://www.nwr.noaa.gov/1sustfsh/efhappendix/page1.html.

Castillo, G. C. (1995). "Latitudinal patterns in reproductive life history traits of northeast pacific flatfish," in *Proceedings of the international symposium on north pacific flatfish* (Fairbanks, AK: Alaska Sea Grant College Program).

Castillo, G. C., Li, H. W., and Golden, J. T. (1993). Environmental induced recruitment variation in petrale sole, eopsetta jordani. *Fish Bull.* 92, 481–493.

Chelton, D. B., Schlax, M. G., and Samelson, R. M. (2011). Global observations of nonlinear mesoscale eddies. *Prog. Oceanogr.* 91, 167–216. doi: 10.1016/j.pocean.2011.01.002

Chelton, D. B., Schlax, M. G., Samelson, R. M., and de Szoeke, R. A. (2007). Global observations of large oceanic eddies. *Geophys Res. Lett.* 34 (L15606). doi: 10.1029/2007GL030812

Cheng, Y. H., Ho, C. R., Zheng, Q., and Kuo, N. J. (2014). Statistical characteristics of mesoscale eddies in the north pacific derived from satellite altimetry. *Remote Sens.* 6, 5164–5183. doi: 10.3390/rs6065164

Chenillat, F., Franks, P. J., Capet, X., Rivière, P., Grima, N., Blanke, B., et al. (2018). Eddy properties in the southern California current system. *Ocean Dyn.* 68, 761–777. doi: 10.1007/s10236-018-1158-4

Combes, V., Chenillat, F., Di Lorenzo, E., Rivière, P., Ohmane, M. D., and Bograd, S. J. (2013). Crossshore transport variability in the California current: ekman upwelling vs. *eddy dynamics. Prog. Oceanogr.* 109, 78–89. doi: 10.1016/j.pocean.2012.10.001

Cooper, D. W., Duffy-Anderson, J. T., Stockhausen, W. T., and Cheng, W. (2013). Modeled connectivity between northern rock sole (Lepidopsetta polyxystra) spawning and nursery areas in the eastern Bering Sea. *J. Sea Res.* 84, 2–12. doi: 10.1016/j.seares.2012.07.001

Curchitser, E. N., Haidvogel, D. B., Hermann, A. J., Dobbins, E., Powell, T. M., and Kaplan, A. (2005). Multi-scale modeling of the north pacific ocean: assessment and analysis of simulated basin-scale variabilit–2003). *J. Geophys Res.* 110 (C11). doi: 10.1029/2005JC002902

Daly, B., Parada, C., Loher, T., Hinckley, S., Hermann, A. J., and Armstrong, D. (2020). Red king crab larval advection in Bristol bay: implications for recruitment variability. *Fish Ocean.* 29 (6), 505–525. doi: 10.1111/fog.12492

Danilson, S., Curchitser, E., Hedstrom, K., Weingartner, T., and Stabeno, P. (2011). On ocean and sea ice modes of variability in the Bering Sea. *J. Geophys Res.* 116 (C12). doi: 10.1029/2011JC007389

Di Donato, G., and Pasquale, N. (1970). Migration of petrale sole tagged in deep water off the Washington coast. *Wash Dept Fish Res. Pap.* 3, 53–61.

Di Lorenzo, E., Mountain, D., Batchelder, H. P., Bond, N., and Hofmann, E. E. (2013). Advances in marine ecosystem dynamics from US GLOBEC: the horizontal-advection bottom-up forcing paradigm. *Oceanogr.* 26 (4), 22–33. doi: 10.5670/oceanog.2013.73

Domenici, P., and Kapoor, B. G. (2010). *Fish locomotion: an eco-ethological perspective* (CRC Press). doi: 10.1201/b10190

Dong, C., Liu, L., Nencioli, F., Bethel, B. J., Liu, Y., Xu, G, et al. (2022). The near-global ocean mesoscale eddy atmospheric-oceanic-biological interaction observational dataset. *Sci. Data* 9, 436. doi: 10.1038/s41597-022-01550-9

Dussin, R., Curchitser, E., Stock, C. A., and Van Oostende, N. (2019). Biogeochemical drivers of changing hypoxia in the California current ecosystem. *Deep-Sea Res. Part II: Topical Stud. Oceanography.* 169–170. doi: 10.1016/j.dsr2.2019.05.013

Eschmeyer, W. N., and Herald, E. S. (1983). *Field guide to pacific coast fishes of north America: from the gulf of Alaska to Baja California (The Peterson field guide series)* (Houghton Mifflin). doi: 10.1086/413730

Fargo, J. (2000). Flatfish stock assessments for the west coast of Canada for 1999 and recommended yield options for 2000. *Can. Sci. Advisory Secretariat Res. Doc.* 99, 199.

Forrester, C. R., and Alderdice, D. F. (1967). Preliminary observations on embryonic development of petrale sole (Eopsetta jordani). *Fish. Res. Board Can. Tech. Rep.* 41, 21.

Fukuhara, O. (1988). Morphological and functional development of larval and juvenile limanda yokohamae (Pisces: pleuronectidae) reared in the laboratory. *Mar. Bio.* 99 (2), 271–281. doi: 10.1007/BF00391990

Gibson, G., Stockhausen, W. T., Coyle, K., Hinckley, S., Parada, C., Hermann, A., et al. (2019). An individual-based model for sablefish: exploring the connectivity between potential spawning and nursery grounds in the gulf of Alaska. *Deep Sea Res. Part II Top. Stud. Oceanogr.* 165, 89–112. doi: 10.1016/j.dsr2.2018.05.015

Giddings, A., Franks, P. J. S., and Baumann-Pickering, S. (2022). Monthly to decadal variability of mesoscale stirring in the California current system: links to upwelling, climate forcing, and chlorophyll transport. *J. Geophys. Res. Oceans* 127, e2021JC018180. doi: 10.1029/2021JC018180

Goldstein, E. D., Pirtle, J. L., Duffy-Anderson, J. T., Stockhausen, W. T., Zimmermann, M., Wilson, M. T., et al. (2020). Eddy retention and seafloor terrain facilitate cross-shelf transport and delivery of fish larvae to suitable nursery habitats. *Limnol. Oceanogr.* 65 2800, 2818. doi: 10.1002/lno.11553

Gregory, P. A., and Jow, T. (1976). The validity of otoliths as indicators of age of petrale sole from California. *California Department Fish Game* 62 (2), 132–140.

Gregory Lough, R., Broughton, E. A., and Kristiansen, T. (2017). Changes in spatial and temporal variability of prey affect functional connectivity of larval and juvenile cod. *ICES J. Mar. Sci.* 74 (6), 1826–1837. doi: 10.1093/icesjms/fsx080

Grioche, A., Harlay, X., Koubbi, P., and Fraga, L. (2000). Vertical migrations of fish larvae: eulerian and Lagrangian observations in the Eastern English channel. *J. Plank Res.* 22 (10), 1813–1828. doi: 10.1093/plankt/22.10.1813

Halo, I., Penven, P., Backeberg, B., Ansorge, I., Shillington, F., and Roman, Y. (2014). Mesoscale eddy variability in the southern extension of the East Madagascar current: seasonal cycle, energy conversion terms, and eddy mean properties. *J. Geophys Res.* 119 (10), 7324–7356. doi: 10.1002/2014JC009820

Haltuch, M. A., Ono, K., and Valero, J. L. (2013). *Status of the U.S. petrale sole resource in 2013* (Portland (OR): Pacific Fishery Management Council).

Haltuch, M. A., Tolimieri, N., Qi, L., and Jacox, M. G. (2020). Oceanographic drivers of petrale sole recruitment in the California current ecosystem. *Fish Ocean.* 29 (2), 122–136. doi: 10.1111/fog.12459

Haltuch, M. A., Wallace, J., Akselrud, C. A., Nowlis, J., Barnett, L. A., Valero, J. L., et al. (2018). *2017 lingcod stock assessment* (Portland, OR: Pacific Fishery Management Council). Available at: http://www.pcouncil.org/groundfish/stock-assessments/.

Hannah, R. W., Parker, S. J., and Fruth, E. L. (2002). Length and age at maturity of female petrale sole (Eopsetta jordani) determined from samples collected prior to spawning aggregation. *U.S. Fish. Bull.* 100, 711–719.

Harry, G. Y. (1959). Time of spawning, length at maturity, and fecundity of the English, petrale, and dover soles (Parophrys vetulus, eopsetta jordani, and microstomus pacificus, respectively). *Fisheries Commission Oregon Res. Briefs.* 7 (1), 5–13.

Hart, J. L. (1973). Pacific fishes of Canada. *Fish Res. Board Can. Bull.* 180, 740.

Hermann, A. J., Curchitser, E. N., Dobbins, E. L., and Haidvogel, D. B. (2009). A comparison of remote versus local influence of El nino on the coastal circulation of the northeast pacific. *Deep Sea Res. Part II Top. Stud. Oceanogr.* 56 (24), 2427–2443. doi: 10.1016/j.dsr2.2009.02.005

Hickey, B. M., and Royer, T. (2001). "California And alaskan currents," in *Encyclopedia of ocean sciences*. Eds. J. H. Steele, S. A. Thorpe and K. A. Turekian (San Diego, California: Academic Press), 368–379.

Hidalgo, M., Rossi, V., Monroy, P., Ser-Giacomi, E., Hernández-García, E., Guijarro, B., et al. (2019). Accounting for ocean connectivity and hydroclimate in fish recruitment fluctuations within transboundary metapopulations. *Ecol. Appl.* 29 (5), e01913. doi: 10.1002/eap.1913

Hinckley, S., Parada, C., Horne, J., Mazur, M., and Woillez, M. (2016). Comparison of individual based model output to data using a model of walleye pollock early life history in the gulf of Alaska. *Deep Sea Res. Part II Top. Stud. Oceanogr.* 132, 240–262. doi: 10.1016/j.dsr2.2016.04.007

Hinckley, S., Stockhausen, W. T., Coyle, K. O., Laurel, B. J., Gibson, G. A., and Parada, C. (2019). Connectivity between spawning and nursery areas for pacific cod (Gadus macrocephalus) in the gulf of Alaska. *Deep Sea Res. Part II Top. Stud. Oceanogr.* 165, 113–126. doi: 10.1016/j.dsr2.2019.05.007

Hoar, W. S., and Randall, D. J. (1978). *Fish physiology, volume VII locomotion* (Academic Press). doi: 10.1016/S1546-5098(08)60157-0

Hoffle, H., Nash, R. D. M., Falkenhaug, T., and Munk, P. (2013). Differences in vertical and horizontal distribution of fish larvae and zooplankton, related to hydrography. *Mar. Biol. Res.* 9 (7), 629–644. doi: 10.1080/17451000.2013.765576

Hufnagl, M., Payne, M., Lacroix, G., Bolle, L. J., Daewel, U., Dickey-Collas, M., et al. (2013). Variation that can be expected when using particle tracking models in connectivity studies. *J. Sea Res.* 127, 133–149. doi: 10.1016/j.seares.2017.04.009

Hurst, T. P., and Abookire, A. A. (2006). Temporal and spatial variation in potential and realized growth rates of age-0 northern rock sole. *J. Fish Biol.* 68, 905–919. doi: 10.1111/j.0022-1112.2006.00985.x

Johnson, A., and Baddeley, A. (2018) *Polyclip: polygon clipping. r package version 1.9-1.* Available at: https://CRAN.R-project.org/package=polyclip.

Johnson, K. F., Taylor, I. G., Langseth, B. J., Stephens, A., Lam, L. S., Monk, M. H., et al. (2021). *Status of lingcod (Ophiodon elongatus) along the southern U.S. west coast in 2021* (Portland (OR: Pacific Fisheries Management Council).

Kapur, M. S., Lee, Q., Correa, G. M., Haltuch, M. A., Gertseva, V., and Hamel, O. S. (2021). *Status of sablefish (Anoplopoma fimbria) along the US West coast in 2021* (Portland (OR: Pacific Fisheries Management Council).

Keister, J. E., and Strub, P. T. (2008). Spatial and interannual variability in mesoscale circulation in the northern California current system. *J. Geophys. Res. Oceans* 113 (C04015). doi: 10.1029/2007JC004256

Keller, A. A., Wallace, J. R., and Methot, R. D. (2017). "The Northwest fisheries science center's West coast groundfish bottom trawl survey: history, design, and description," in *NOAA Technical memorandum NMFS-NWFSC-136* (U.S. Department of Commerce). doi: 10.7289/V5/TM-NWFSC-136

Kerr, L. A., Hintzen, N. T., Cadrin, S. X., Clausen, L. W., Dickey-Collas, M., Goethel, D. R., et al. (2017). Lessons learned from practical approaches to reconcile mismatches between biological population structure and stock units of marine fish. *ICES J. Mar. Sci.* 74 (6), 1708–1722. doi: 10.1093/icesjms/fsw188

Ketchen, K. S., and Forrester, C. R. (1966). Population dynamics of the petrale sole, eopsetta jordani, in waters off western Canada. *Fish Res. Bd Canada Bull.* 115, 195.

Kurian, J., Colas, F., Capet, X., McWilliams, J. C., and Chelton, D. B. (2011). Eddy properties in the California current system. *J. Geophys. Res.* 116, C08027. doi: 10.1029/2010JC006895

Lacroix, G., Barbut, L., and Volckaert, F. A. M. (2017). Complex effect of projected sea temperature and wind change on flatfish dispersal glob. *Change Biol.* 24 (1), 85–100. doi: 10.1111/gcb.13915

Lanksbury, J. A., Duffy-Andreson, J. T., Mier, K. L., Busby, M. S., and Stabeno, P. J. (2007). Distribution and transport patterns of northern rock sole, lepidopsetta polyxystra, larvae in the southeastern Bering Sea. *Prog. Oceanogr.* 72 (1), 39–62. doi: 10.1016/j.pocean.2006.09.001

Lefebvre, L. S., Friedlander, C. L., and Field, J. C. (2019). Reproductive ecology and size-dependent fecundity in the petrale sole, eopsetta jordani, in waters of California, Oregon and Washington. *Fish. Bull.* 117, 291–302. doi: 10.7755/FB.117.4.2

Lett, C., Verley, P., Mullon, C., Parada, C., Brochier, T., Pierrick, P., et al. (2008). A Lagrangian tool for modelling ichthyoplankton dynamics. *Environ. Model. Software* 23 (9), 1210–1214. doi: 10.1016/j.envsoft.2008.02.005

Lindgren, F., and Rue, H. (2015). Bayesian Spatial modelling with r-INLA. *J. Stat. Software* 63 (19), 1–25. doi: 10.18637/jss.v063.i19

Love, M. (1996). *Probably more than you want to know about the fishes of the pacific coast* (Really Big Press). Availble at: https://cir.nii.ac.jp/crid/1130000798159712000.

Marchesiello, P., McWilliams, J. C., and Shchepetkin, A. (2003). Equilibrium structure and dynamics of the California current system. *J. Phys. Oceanogr.* 33, 753–783. doi: 10.1175/1520-0485(2003)33<753:ESADOT>2.0.CO;2

Megrey, B. A., and Hinckley, S. (2001). Effect of turbulence on feeding of larval fishes: a sensitivity analysis using an individual-based model. *ICES J. Mar. Sci.* 58 (5), 1015–1029. doi: 10.1006/jmsc.2001.1104

Miller, D. D., Ota, Y., Sumaila, U. R., Cisneros-Montemayor, A. M., and Cheung, W. W. (2018). Adaptation strategies to climate change in marine systems. *Glob Chang Biol.* 24 (1), e1–e14. doi: 10.1111/gcb.13829

Moser, H. G. (1996). "The early stages of fishes in the California current region," in *California Cooperative oceanic fisheries investigations, atlas no. 33* (Allen Press, Inc). Availble at: https://calcofi.org/downloads/publications/atlases/CalCOFI_Atlas_33.pdf.

Okubo, A. (1970). Horizontal dispersion of floatable particles in the vicinity of velocity singularities such as convergences. *Deep-Sea Res.* 17, 445–454. doi: 10.1016/0011-7471(70)90059-8

Ospina-Álvarez, A., Parada, C., and Palomera, I. (2012). Vertical migration effects on the dispersion and recruitment of European anchovy larvae: from spawning to nursery areas. *Ecol. Modell.* 231, 65–79. doi: 10.1016/j.ecolmodel.2012.02.001

Pacific Fisheries Information Network (PacFIN) (2016) (Portland, Oregon: Pacific States Marine Fisheries Commission). Available at: www.psmfc.org.

Palacios-Abrantes, J., Reygondeau, G., Wabnitz, C. C., and Cheung, W. W. (2020b). The transboundary nature of the world's exploited marine species. *Sci. Rep.* 10, 17668. doi: 10.1038/s41598-020-74644-2

Palacios-Abrantes, J., Sumaila, U. R., and Cheung, W. W. (2020a). Challenges to transboundary fisheries management in north America under climate change. *Ecol. Soc* 25 (4), 41. doi: 10.5751/ES-11743-250441

Parada, C., Armstrong, D. A., Ernst, B., Hinckley, S., and Orensanz, J. M. (2010). Spatial dynamics of snow crab (Chionoecetes opilio) in the eastern Bering Sea – putting together the pieces of the puzzle. *Bull. Mar. Sci.* 86 (2), 413–437.

Parada, C., Hinckley, S., Horn, J., Mazur, M., Hermann, A., and Curchister, E. N. (2016). Modeling connectivity of walleye pollock in the gulf of Alaska: are there any

linkages to the Bering Sea and Aleutian islands? *Deep Sea Res. Part II Top. Stud. Oceanogr.* 132, 227–239. doi: 10.1016/j.dsr2.2015.12.010

Pearcy, W. G., Hosie, M. J., and Richardson, S. L. (1977). Distribution and duration of pelagic life of larvae of Dover sole, microstomus pacificus; rex sole, glyptocephalus zachirus; and petrale sole eopsetta jordani, in waters off Oregon. *Fish Bull.* 75, 173–183.

Pedersen, M. G. (1975). Movements and growth of petrale sole (Eopsetta jordani) tagged off Washington and southwest Vancouver island. *J. Fish Res. Board Can.* 32 (1), 2169–2177. doi: 10.1139/f75-255

Penven, P., Echevin, V., Pasapera, J., Colas, F., and Tam, J. (2005). Average circulation, seasonal cycle, and mesoscale dynamics of the Peru current system: a modeling approach. *J. Geophys Res.* 110 (C10). doi: 10.1029/2005JC002945

PFMC (2019). *Pacific coast groundfish fishery management plan for the California, Oregon, and Washington groundfish fishery appendix b part 2: groundfish essential fish habitat and life history descriptions, habitat use database description, and habitat suitability probability information* (Portland (OR: Pacific Fishery Management Council).

Politikos, D., Curchitser, E. N., Rose, K., Checkley, D., and Fiechter, J. (2018). Climate variability and sardine recruitment in the California current: a mechanistic analysis of an ecosystem model. *Fish Oceanog.* 27 (6), 602–622. doi: 10.1111/fog.12381

Politikos, D., Somarakis, S., Tsiarasa, K. P., Giannoulaki, M., Petihakis, G., Machias, A., et al. (2015). Simulating anchovy's full life cycle in the northern Aegean Sea (eastern mediterranean): a coupled hydro-biogeochemical–IBM model. *Prog. Oceanogr* 138, 399–416. doi: 10.1016/j.pocean.2014.09.002

Porter, P. (1964). *Notes on fecundity, spawning, and early life history of petrale sole (Eopsetta jordani), with descriptions of flatfish larvae collected in the pacific ocean off Humboldt bay, california. M.S.thesis* (Humboldt State College), 98. Available at: https:// science-catalogue.canada.ca/record=3854905~S6.

Powell, A., Clarke, M. E., Haltuch, M. A., Fruh, E., Anderson, J., Whitmire, C. E., et al. (2022). First autonomous underwater vehicle observations of a potential petrale sole (Eopsetta jordani) spawning aggregation off the US West coast. *Front. Mar. Sci.* 9. doi: 10.3389/fmars.2022.834839

Ramesh, N., Rising, J. A., and Iremus, K. L. (2019). The small world of global marine fisheries: the cross-boundary consequences of larval dispersal. *Science.* 364 (6446), 1192–1196. doi: 10.1126/science.aav3409

Rodgveller, C. J., Stark, J. W., Echave, K. B., and Hulson, P. F. (2016). Age at maturity, skipped spawning and female sablefish (Anoplopoma fimbria) during the spawning season. *Fish Bull.* 114, 89–102. doi: 10.7755/FB

Sadorus, L. L., Goldstein, E. D., Webster, R. A., Stockhausen, W. T., Planas, J., and Duffy-Anderson, J. T. (2020). Multiple life-stage connectivity of pacific halibut (Hippoglossusstenolepis) across the Bering Sea and gulf of Alaska. *Fish. Oceanogr.* 30, 174–193. doi: 10.1111/fog.12512

Santora, J. A., Mantua, N. J., Schroeder, I. D., Field, J. C., Hazen, E. L., Bograd, S. J., et al. (2020). Habitat compression and ecosystem shifts as potential links between marine heatwave and record whale entanglement. *Nat. Commun.* 11, 536. doi: 10.1038/s41467-019-14215-w

Scheffer, M., Baveco, J. M., DeAngelis, D. L., Rose, K. A., and van Nes, E. H. (1995). Super-individuals a simple solution for modelling large populations on an individual basis. *Ecol. Modell.* 80 (2–3), 161–170. doi: 10.1016/0304-3800(94)00055-M

Schroeder, I. D., Leising, A., Bograd, S., deWitt, L., Garfield, N., Hazen, E. L., et al. (2021). "Climate and ocean drivers," in *Ecosystem status report of the California current for 2020–21: a summary of ecosystem indicators compiled by the California current integrated ecosystem assessment team (CCIEA).* Eds. C. J. Harvey, N. Garfield, G. D. Williams and N. Tolimieri (U.S. Department of Commerce), 8–28. doi: 10.25923/x4ge-hn11

Seo, H., Miller, A. J., and Norris, J. R. (2015). Eddy-wind interaction in the California current system: dynamics and impacts. *J. Phys. Oceanogr.* 46, 439–459. doi: 10.1175/JPO-D-15-0086.1

Sogard, S. M., Berkeley, S. A., and Fisher, R. (2008). Maternal effects in rockfishes sebastes spp.: a comparison among species. *Mar. Ecol. Prog. Ser.* 360, 227–236. doi: 10.3354/meps07468

Starr, P. J. (2009). "Petrale sole (Eopsetta jordani) in British Columbia, Canada: stock assessment for 2006/7 and advice to managers for 2007/8," in *Canadian Science advisory secretariat research document 2009/70.* Available at: https://waves-vagues. dfo-mpo.gc.ca/library-bibliotheque/339143.pdf.

Starr, P. J., and Fargo, J. (2004). Petrale sole stock assessment for 2003 and recommendations for management in 2004. *CSAS Res. Doc.* 2004, 036.

Stawitz, C. C., Hurtado-Ferro, F., Kuriyama, P. T., Trochta, J., Johnson, K. F., Haltuch, M. A., et al. (2015). *Stock assessment update: status of the U.S. petrale sole resource in 2014* (Portland (OR: Pacific Fishery Management Council).

Stockhausen, W. T., Coyle, K. O., Hermann, A. J., Blood, D., Doyle, M. J., Gibson, G. A., et al. (2019). Running the gauntlet: connectivity between spawning and nursery areas for arrowtooth flounder (Atheresthes stomias) in the gulf of Alaska, as inferred from a biophysical individual-based model. *Deep Sea Res. Part II Top. Stud. Oceanogr.* 165, 127–139. doi: 10.1016/j.dsr2.2018.05.017

Sumaila, U. R., Cheung, W. W., Lam, V. W. Y., Pauly, D., and Herrick, S. (2011). Climate change impacts on the biophysics and economics of world fisheries. *Nat. Climate Change* 1 (9), 449–456. doi: 10.1038/nclimate1301

Thebaud, O. (1997). Transboundary marine fisheries management. recent developments and elements of analysis. *Mar. Policy.* 21 (3), 237–253. doi: 10.1016/S0308-597X(97)00005-5

Thorson, J. T. (2018). Three problems with the conventional delta-model for biomass sampling data, and a computationally efficient alternative. *Can. J. Fish Aquat Sci.* 75 (9), 1369–1382. doi: 10.1139/cjfas-2017-0266

Thorson, J. T. (2019). Guidance for decisions using the vector autoregressive spatio-temporal (VAST) package in stock, ecosystem, habitat and climate assessments. *Fish Res.* 210, 143–161. doi: 10.1016/j.fishres.2018.10.013

Thorson, J. T., and Barnett, L. A. K. (2017). Comparing estimates of abundance trends and distribution shifts using single- and multispecies models of fishes and biogenic habitat. *ICES J. Mar. Sci.* 74 (5), 1311–1321. doi: 10.1093/icesjms/fsw193

Tolimieri, N., Haltuch, M. A., Lee, Q., Jacox, M. G., and Bograd, S. J. (2018). Oceanographic drivers of sablefish recruitment in the California current. *Fish Ocean.* 27 (5), 458–474. doi: 10.1111/fog.12266

Tolimieri, N., Wallace, J., and Haltuch, M. A. (2020). Spatio-temporal patterns in juvenile habitat for 13 groundfishes in the California current ecosystem. *PloS One* 15 (8), e0237996. doi: 10.1371/journal.pone.0237996

Verheijen, F. J., and deGroot, S. J. (1966). Diurnal activity of plaice and flounder (Pleuronectidae) in aquaria. *Neth J. Sea Res.* 3, 383–390. doi: 10.1016/0077-7579(67)90011-7

Weiss, J. (1991). The dynamics of enstrophy transfer in two-dimensional hydrodynamics. *Physica D.* 48, 273–294. doi: 10.1016/0167-2789(91)90088-Q

Wetzel, C. R. (2019). *Status of petrale sole (Eopsetta jordani) along the U.S. west coast in 2019* (Portland (OR: Pacific Fishery Management Council).